Permafrost and Periglacial Processes, Vol. 8: 409–426 (1997)

Analysing the Creep of Mountain Permafrost using High Precision Aerial Photogrammetry: 25 Years of Monitoring Gruben Rock Glacier, Swiss Alps

A. Kääb,[1]* *W. Haeberli*[2] *and G. Hilmar Gudmundsson*[1]

[1]Laboratory of Hydraulics, Hydrology and Glaciology (VAW), ETH, 8092 Zurich, Switzerland
[2]Department of Geography, University of Zurich, Winterthurerstrasse 190, 8057 Zurich, Switzerland

ABSTRACT

Aerophotogrammetrical monitoring of Gruben rock glacier over the period 1970 to 1995 results in a unique time series documenting the three-dimensional surface kinematics of creeping mountain permafrost. In places, the area under study is affected by historical fluctuations of the polythermal Gruben glacier. Changes in elevation and surface velocities were measured over five consecutive five-year periods using an advanced photogrammetric monoplotting technique of multitemporal stereo models. The measurements are based on a regular grid with a mesh width of 25 metres and have an accuracy of a few centimetres per year. Although surface lifting occurred in places and within individual time intervals, surface subsidence predominated at an average rate of a few centimetres per year in the 'periglacial' part of the rock glacier and of a few decimetres per year in the 'glacier-affected' part of the rock glacier which still contains some dead glacier ice in permafrost. Fluctuations in horizontal surface velocities seem to correlate with temporal changes in surface elevation. Analysing flow along principal trajectories and interpreting the advance rate of the front leads to an age estimate of the rock glacier of a few millennia. Dynamic effects of three-dimensional straining within the creeping permafrost as computed from the measured surface velocity field are estimated to potentially contribute to surface heave or subsidence in the same order of magnitude as the observed vertical changes. Temporal variations of surface altitudes at Gruben rock glacier show distinct similarities with mass balance and surface altitude variations determined on nearby glaciers but at a greatly reduced amplitude. This similarity may indicate that the same climatic forcing (summer temperatures?) could possibly have a predominant influence on permafrost aggradation/degradation as well as on glacier mass balance in mountain areas. © 1997 John Wiley & Sons, Ltd.

RÉSUMÉ

Le suivi aérophotogrammétrique du glacier rocheux de Gruben pendant la période de 1970 à 1995 a donné une série unique d'observations qui ont permis de préciser en trois dimensions la cinématique du creep du pergélisol de montagne. La zone étudiée a permis aussi de suivre les fluctuations historiques du glacier Gruben. Des changements en altitude et des vitesses de surface ont été mesurées au cours de 5 périodes de 5 ans, en utilisant une technique avancée pour étudier les modèles stéréoscopiques multitemporels. Les mesures ont été effectuées avec une précision de quelques centimètres par an selon une grille régulière ayant une maille de 25 mètres. Bien que des soulèvements de surface se produisent localement et temporairement, des phénomènes de subsidence prédominent. Ils ont une valeur moyenne de quelques centimètres par an dans la

* Correspondence to: Dr A. Kääb, Department of Geography, University of Zurich, Winterthurerstrasse 190, 8057 Zurich, Switzerland. e-mail: kaeaeb@geo.unizh.ch

Contract grant sponsor: Swiss National Science Foundation

CCC 1045–6740/97/040409–18$17.50

Received 21 August 1997
Revised 19 October 1997
Accepted 20 October 1997

partie périglaciaire du glacier rocheux et de quelques décimètres par an dans la partie où de la glace d'origine glaciaire est comprise dans le pergélisol. Les variations des vitesses horizontales de surface paraissent se corréler avec les variations verticales de celle-ci. L'analyse de l'écoulement le long des trajectoires principales et l'interprétation de l'avancée du front conduisent à estimer l'âge du glacier rocheux à quelques milliers d'années. Les effets dynamiques des contraintes en trois dimensions qui déforment le pergélisol (telles qu'elles sont calculées à partir du champ des vitesses de surface) peuvent potentiellement contribuer à expliquer des mouvements de soulèvement et de subsidence du même ordre de grandeur que les mouvements verticaux observés. Les variations temporelles des altitudes de surface du glacier rocheux de Gruben montrent des similarités distinctes des variations de masse et des altitudes de surface déterminées sur des glaciers proches mais avec cependant une amplitude considérablement réduite. Cette similarité peut indiquer que le même effet climatique (les températures d'été?) ont une influence prédominante sur les phénomènes d'aggradation et de dégradation du pergélisol comme cela est connu pour les balances de masses glaciaires des régions montagneuses. © 1997 John Wiley & Sons, Ltd.

Permafrost Periglac. Process., Vol. 8: 409–426 (1997).
(No. of Figs: 17. No. of Tables: 0. No. of Refs: 31.)

KEY WORDS: rock glacier; photogrammetry; monitoring; creep velocity; deformation

INTRODUCTION

Rock glaciers represent typical phenomena of steady ice and debris transport in the permafrost of cold mountain areas. Negative subsurface temperatures and generally high ice contents within the creeping mountain permafrost lead to characteristic spatial surface velocities of centimetres, decimetres and sometimes up to a few metres per year. Temporal changes in ground ice conditions generally involve strong effects from latent heat exchange coupled with slow and delayed heat diffusion processes and correspondingly weak heat fluxes. The resulting thermal inertia with low rates of freezing and thawing at the permafrost table and the permafrost base stabilize boundary conditions, so that the geometry and flow regime of perennially frozen ground on mountain slopes change slowly with time. Thus, they are mainly affected by long-term climatic trends. Analysis of small permafrost creep rates, and their temporal as well as spatial variations, requires the application of precise high-resolution techniques. Long-term monitoring is necessary for accurately documenting slow temporal changes in geometry and flow (Wagner, 1992; 1996). As demonstrated by numerous earlier studies, aerophotogrammetry represents a powerful remote sensing tool for measuring geometrical changes of alpine permafrost surfaces (e.g. Messerli and Zurbuchen, 1968; Barsch and Hell, 1976; Haeberli *et al.*, 1979; Evin and Assier, 1982; Haeberli and Schmid, 1988; Vonder Mühll and Schmid, 1993; Kaufmann, 1996).

Large-scale aerial photographs have been taken annually by the Federal Office of Cadastral Surveys since 1970 at the Gruben locality in connection with the monitoring of dangerous periglacial lakes. A recent investigation as part of the Swiss National Research Programme 31 'Climate Changes and Natural Disasters' successfully applied photogrammetric techniques for early recognition and prevention of flood and debris-flow hazards constituted by the growth of these lakes on and around the Gruben rock glacier and the nearby Gruben glacier (Kääb and Haeberli, 1996; Kääb *et al.*, 1996). The availability of excellent photogrammetric material enabled the study of creep processes and the monitoring of long-term geometric developments within perennially frozen sediments and massive ground ice of the large active Gruben rock glacier. Shallow core drilling, geophysical investigations and lichen-cover studies (Barsch *et al.*, 1979; Haeberli, 1985; Haeberli *et al.*, 1979; King *et al.*, 1987) have been carried out giving valuable support to the photogrammetric observations. With its exceptionally long and detailed photogrammetric record, Gruben rock glacier is now an important part of the permafrost monitoring network in the Swiss Alps (Haeberli *et al.*, 1993), which aims to document changes in mountain permafrost conditions as related to climatic forcing.

Results from the aerophotogrammetric monitoring of the Gruben rock glacier for the period 1970 to 1979 were published by Haeberli and Schmid (1988), and for the period 1970 to 1991 by Haeberli

Figure 1 Gruben rock glacier (left) and Gruben glacier (right) (1985, photo W. Schmid).

et al. (1993). In this paper, data are presented on the geometrical development of the creeping rock glacier permafrost from 1970 to 1995. In addition, new results from analysing creep rates and strain fields are discussed. For that purpose, the whole photogrammetric time-series was remeasured using a newly developed, more precise technique.

SITE DESCRIPTION

Gruben glacier, Wallis, Swiss Alps, flows from the peak of Fletschhorn (3993 m ASL) between the Saas valley and the Simplon pass (Figure 1) down to a well-developed cirque. Within this cirque and roughly parallel to the orographic right side of the polythermal Gruben glacier tongue, Gruben rock glacier developed at an altitude of about 2900 m ASL within thick accumulations of periglacial debris and morainic material in an environment of discontinuous mountain permafrost (Figures 2 and 3). A number of periglacial lakes are located at the margin, as well as in front of the glacier tongue and on the rock glacier itself. In both 1968 and 1970, outburst floods from glacier-dammed lake 3 in the contact zone between the glacier tongue and the rock glacier caused damage in the nearby village of Saas Balen. In order to prevent further floods and debris flows, geophysical and geodetic investigations were carried out, aerophotogrammetric monitoring was started, a protective plan was devised and corresponding construction work was undertaken (Röthlisberger, 1979; Kääb and Haeberli, 1996; Vonder Mühll *et al*., 1996).

During its Holocene and historical advances, Gruben glacier must have repeatedly overridden the upper part of the rock glacier (Haeberli *et al*., 1979). During glacier retreat periods, debris-covered dead ice was deposited on top of the rock-glacier permafrost, affecting the dynamics of the rock glacier in its upper and orographic left part (Figure 4). In the following, this part of the creeping permafrost body is called the *glacier-affected part*, whereas the lower and orographic right part, not directly influenced by recent glacier activity, is called the *periglacial part*.

Characteristic mean annual surface temperatures of the rock glacier are close to $-1\,^{\circ}C$ today. The thickness of the relatively warm permafrost may still be influenced by ground thermal conditions during the somewhat colder past centuries (Haeberli, 1985). The thickness is known to be up to 100 and more metres in the periglacial part, and characteristically a few tens of metres in the glacier-affected part (Haeberli, 1985; King *et al*., 1987). In the periglacial part of the rock glacier, a transverse bedrock riegel was detected at a depth of 30 metres below surface (unpublished seismic refraction soundings, cf. Figure 8).

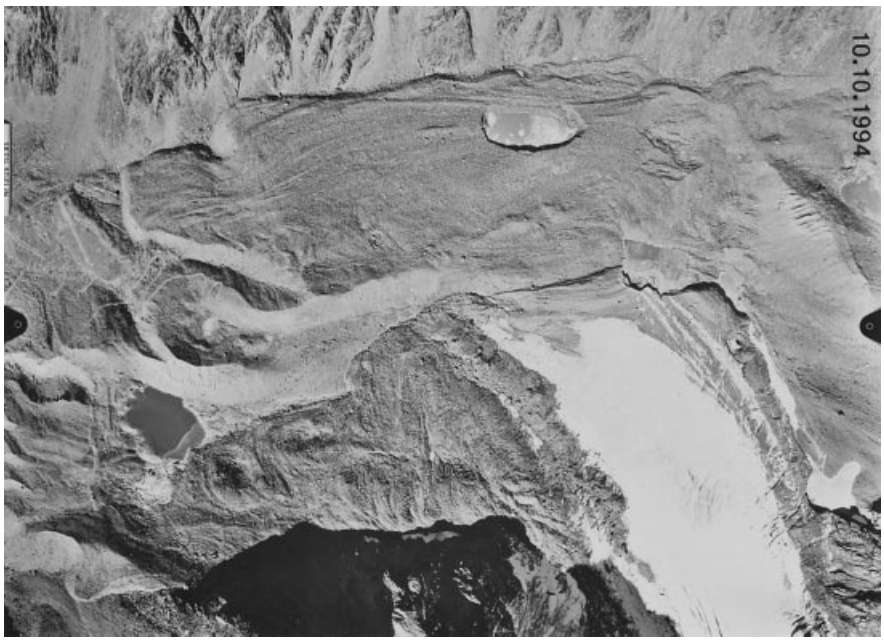

Figure 2 Gruben rock glacier (top), tongue of Gruben glacier (bottom) and periglacial lakes (aerial photo taken by Federal Office of Cadastral Surveys).

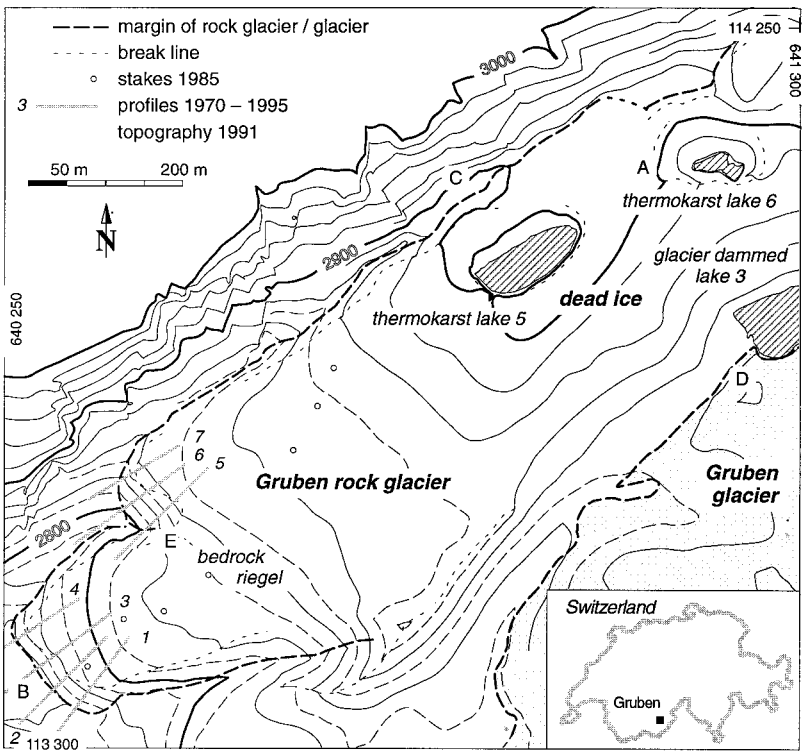

Figure 3 Map of Gruben rock glacier and its location in Switzerland. Letters A–E and numbers 1–7 referred to in Figures 8 and 16

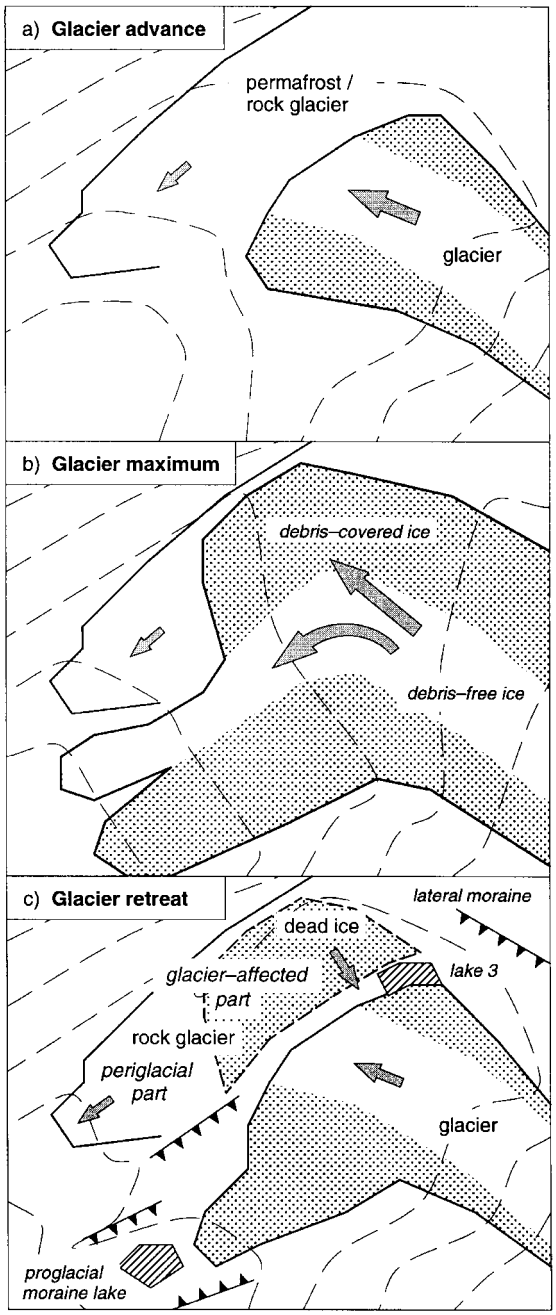

Figure 4 Schematic diagram illustrating how Holocene advances and retreats of the Gruben glacier affect the rock glacier.

In the mid 1960s, two crevasses formed at the upper margin of dead ice occurrences within the rock glacier permafrost. These two surface depressions filled with water and progressively enlarged by thermal convection. This led to intensified melting of the dead glacier ice and probably also of ice contained within underlying permafrost. One of these two thermokarst lakes, lake 6, only fills up during winter and spring. In late autumn, freezing water seals the lake bottom. Subsequently, the lake fills with snow, water and ice until the next melting season starts. When the lake is completely full of water, the frozen bottom leaks and the lake slowly empties by draining through either remaining dead ice layers or underlying permafrost. In contrast, the permafrost and dead ice damming the other thermokarst lake, lake 5, appear to be impermeable and the water level remains nearly stable throughout the year. In 1994, lake 5 had a surface area of about 10,000 m^2 and a volume (determined by sonar soundings) of about 50,000 m^3. Its annual area and volume growth rate reached values of 1500 m^2 and 7500 m^3, respectively (Kääb *et al.*, 1996; cf. Haeberli, 1980). In view of the increasing risk of a lake outburst, again endangering the village of Saas Balen, most of the water within this thermokarst lake was pumped out in summer 1995 as part of the flood protection plan for the whole Gruben area (Kääb *et al.*, 1996). It is planned to keep the future water level low by an open ditch. Based on results from aerophotogrammetric analyses of potential hazards from such lakes, additional flood protection measures were taken at the glacier margin. The water level of lake 3, situated at a retreating calving front of the glacier, was lowered and regulated by the excavation of a ditch in summer 1996. The remaining lake volume was largely filled up with the excavated debris. The artificial outlet of the moraine lake in front of the glacier tongue was stabilized by concrete injections and deepened in order to increase its water retention capacity.

PHOTOGRAMMETRIC METHODS

Changes in surface elevation of creeping mountain permafrost are caused by the sum of (a) sediment accumulation/evacuation, (b) three-dimensional deformation (extension/compression) and (c) terrain subsidence caused by either thawing of supersaturated permafrost or frost heave due to freezing of water. As a complex function of sediment accumulation at the surface, flow from higher to lower altitudes and cumulative vertical straining of supersaturated permafrost, thawing and freezing can take place either at the permafrost table, or within the permafrost body, or at the

permafrost base (cf. Haeberli and Vonder Mühll, 1996). Vertical displacements are the result of spatial/dynamic processes. Thus, determination of surface displacements in full three dimensions is necessary for better understanding the physical processes involved.

Aerophotogrammetric determination of digital terrain models (DTMs) and subsequent comparison of multitemporal DTMs is an effective and well-established technique to exactly define terrain surfaces and their temporal changes in elevation. The method uses monotemporal stereo models, composed by at least two overlapping photographs which are taken from different places. The terrain point A (see Figure 5) is computed by intersecting two spatial rays, each fixed by the known projection centres and the projections $A'_1(t_1)$ and $A'_2(t_1)$ of the selected terrain point. Repeating the procedure at other points gives a DTM of time t_1, and repeating the procedure using photographs taken at time t_2 gives point B respectively a DTM of time t_2 and – by comparison of two DTMs – the area-wide changes in surface elevation.

With respect to surface displacements, a new high-precision photogrammetric method was developed and applied, based on earlier concepts published by Finsterwalder (1931), Hofmann (1958), Grün and Sauermann (1977), Flotron (1979), Saksono (1984) and Armenakis (1984) and translated into a programme for a computer-aided photogrammetric compilation system (analytical plotter) (Kääb, 1996). The method uses multitemporal stereo models composed by aerial photographs taken at different times and from different places (e.g. photo 1 (t_2) and photo 2 (t_1) in Figure 5).

Between time t_1 and time t_2 the point A has moved to point C, passively riding on the moving surface. A block or a stone on the surface of the creeping permafrost could, for instance, be a suitable target. The projection $A'_2(t_1)$ of such a point is chosen from the photograph taken at time t_1. Intersecting the spatial ray fixed by this image point and the known projection centre with the terrain surface represented by the DTM of time t_1 gives the ground coordinates of point A. This procedure is called monoplotting. The image point C'_1 at time t_2, $C'_1(t_2)$, which corresponds to $A'_2(t_1)$, can now be found using the stereoscopic overlap. The operator thereby cancels the terrain movement which has occurred between the times t_1 and t_2 by displacing one image while simultaneously looking at the multitemporal photographs. This simultaneous and stereoscopic observation supports the identification of corresponding points, improves the accuracy of the measurements and, additionally, indicates whether a local displacement reflects in a significant way its surrounding terrain. In the same way as for the spatial position of point A, the position of point C is computed by monoplotting. Thus, spatial displacements of surface points can be deduced area-wide.

The terrain surface of which the velocity field shall be determined has to fulfil basic requirements:

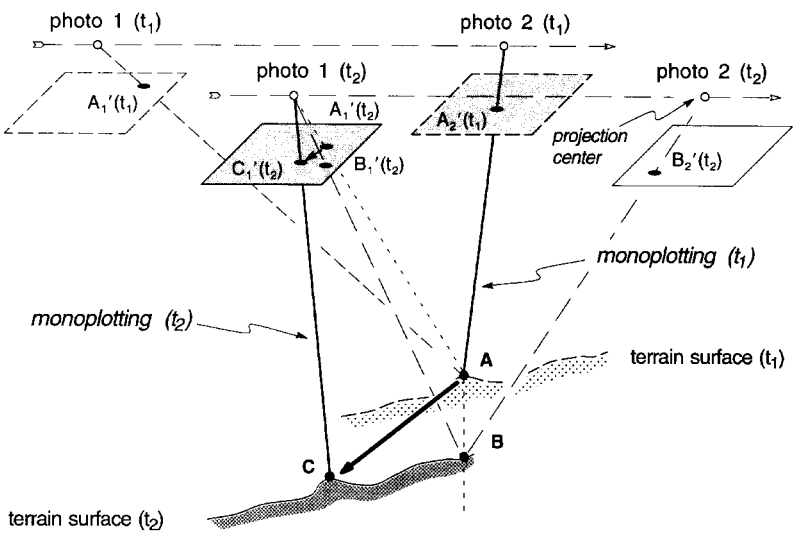

Figure 5 Monotemporal photogrammetric stereo models are used to determine surface elevation and its changes. Using multitemporal stereo models composed by photographs taken at different times from different places, surface displacements can be measured as well.

(1) the terrain has to show corresponding features at every time of photography; (2) the displacements must be larger than the accuracy of the method to obtain significant results; and (3) terrain changes between the times of photography, e.g. caused by thawing or terrain slip, should not prohibit the identification of corresponding points. Requirements (2) and (3) can be satisfied by choosing a suitable time interval between the photo missions. The photogrammetric technique described here works especially well for determining the creep of permafrost surfaces and is also suitable for observing glacier flow and slope movements (Kääb, 1996). Owing to requirement (1) it is not possible to determine displacements of snow-covered terrain. Maximum accuracy of the method is assumed to be about ± 30 μm in image scale or, in the case of the photogrammetric parameters of the Gruben missions, about ± 0.2 m on the ground. The actual accuracy of the displacements measured photogrammetrically can be deduced by repeating measurements using independent multitemporal stereo models and by comparing the results with geodetic stake measurements. The error (root mean square) of the displacement measurements on Gruben rock glacier is about ± 0.4 m or, in the case of a five-year interval between two photo missions, about ± 0.08 m per year (m/a).

SURFACE ELEVATION

In order to determine changes in surface elevation of Gruben rock glacier between 1970 and 1995, DTMs of 1970, 1975, 1979, 1985, 1991 and 1995 were measured photogrammetrically (time of photography was autumn in every case). A measuring interval of about five years was chosen on the basis of results from earlier velocity and altitude change determinations at the rock glacier surface. Unfavourable terrain and flying conditions in 1980 and 1990 prevented keeping exact five-year intervals throughout the entire observation period. Each of the six DTM grids has a regular grid distance of 25 m. (Horizontal displacements were later measured at the same DTM points). The changes in surface elevation deduced from the vertical differences between identical grid points in corresponding DTMs were smoothed by the Gaussian low-pass filter. This procedure reduces the data noise without causing a systematic elevation shift. Figure 6 shows the average

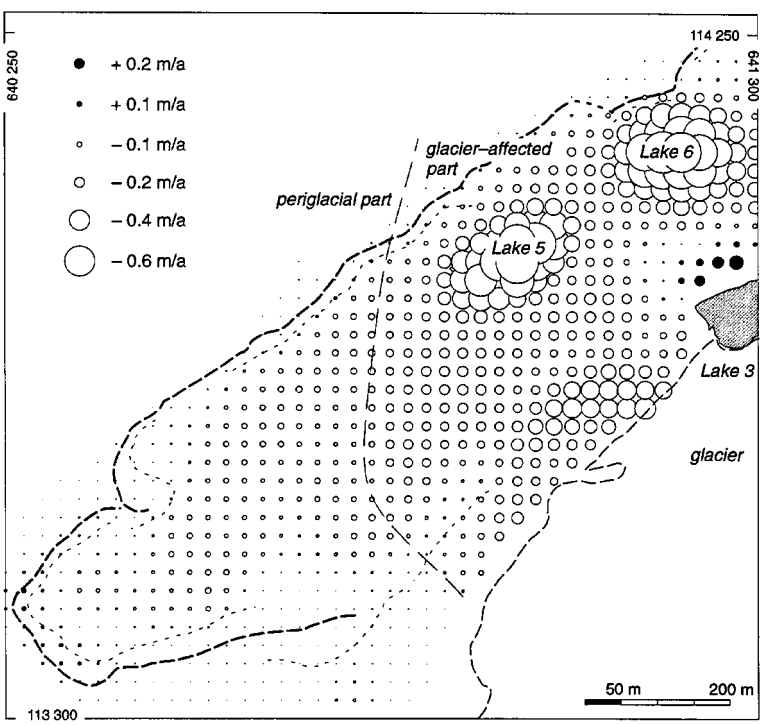

Figure 6 Changes in surface elevation of the Gruben rock glacier, 1970–95.

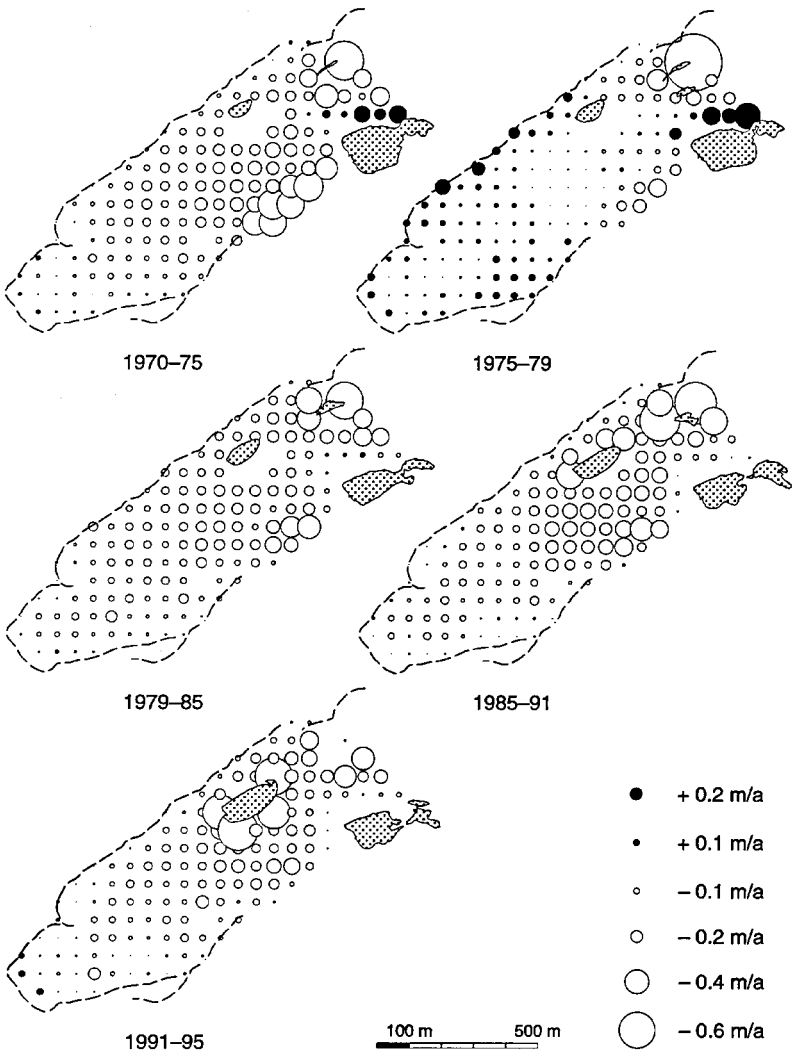

Figure 7 Vertical velocities at about five-year intervals. Lakes indicated are those at the end of the measurement period.

changes in surface elevation between 1970 and 1995; Figure 7 shows the individual five-year variations thinned out for a 50 m grid. The surface profiles are shown in Figure 8, and the changes in the vertical displacement rates between the individual five-year time intervals are presented in Figure 9.

Between 1970 and 1995 the periglacial part of the Gruben rock glacier showed a total surface lowering of about −0.05 m/a on average with maxima reaching −0.10 m/a and more in the central parts. On the other hand, the average loss in surface elevation of the glacier-affected part containing remains of dead ice is about −0.20 m/a during the same period. The higher ice content of the dead ice (about 100%), in contrast to the lower ice content of the perennially frozen debris (about 50–70%; Barsch *et al.*, 1979), probably causes the observed higher subsidence rates. Thus, the two parts of the rock glacier, i.e. the periglacial and the glacier-affected area, clearly differ with respect to temporal changes in surface elevation (Figure 6).

Specific details of the area-wide changes in surface elevation are illustrated in Figures 6 and 7. The formation and fast growth of the thermokarst lakes described above (cf. Figure 3) brought about large losses of ice, inducing pronounced surface lowering at lakes 5 and 6. The retreat of the glacier ice margin, which prevailed during the period 1970 to 1995 and the years before, caused an important

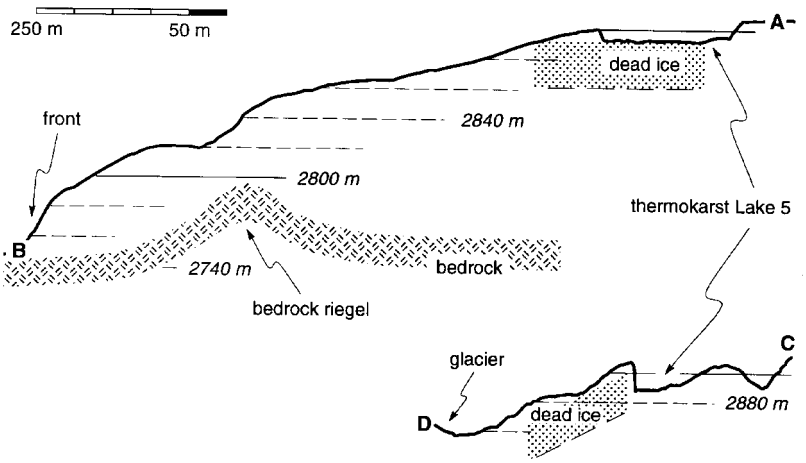

Figure 8 Surface profiles in south-western and south-eastern directions. Two times vertical exaggeration. Start and end points A–D, see Figure 3. Bedrock and dead ice layer are schematically indicated.

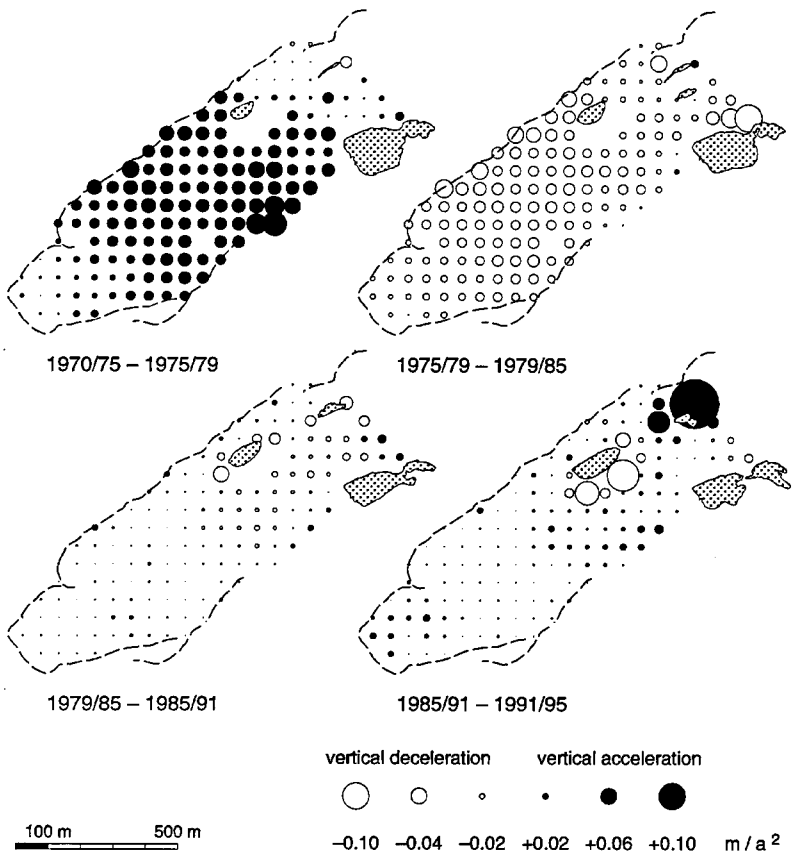

Figure 9 Variations with time of changes in surface elevation, Gruben rock glacier.

but decelerating surface lowering to the south-west of lake 3 in the zone of direct contact between the glacier and the rock glacier (Figure 9). Between this area and thermokarst lake 5, changes in elevation show gradual spatial variation. This may indicate different thicknesses of the insolating debris cover from active layer adjustment over increasing time periods and, thus, different effects from former

glacier overriding (cf. Figure 8, bottom). Dynamic effects from compression and extension of the ice/debris mixture and the surface-debris layer due to the flowing of the entire mass towards the topographic depression left by the retreating glacier may also play a role. Such dynamic effects obviously take place in the case of the surface rise to the north-west of the glacier-dammed lake 3. Under the influence of enhanced energy influx from solar radiation and warm lake water, the dead ice originally existing in that area may already have melted away to a large degree as indicated by the relatively stable lake border at the foot of the corresponding slope. In fact, the remaining debris may have started slowing down the flow of the ice/debris mixture towards the lake and, hence, caused horizontal compression and surface uplift. Near the rock glacier front, the relatively stable, or slightly rising, surface altitude can be explained by the advance of the creeping permafrost, as discussed below.

The changes in the rates of height variation (Figure 9) have been calculated as differences between the average annual changes in elevation. While individual acceleration values are hardly significant owing to the accuracy of single elevation measurements, the spatial distribution shows a clear pattern. Thus, Figure 9 makes clear the differences between the changes in surface elevation of the five-year intervals, shown in Figure 7. For instance, between 1970–75 and 1975–79 the vertical surface velocities were increasing (accelerating) in most parts. In other words, surface lowering diminished from 1970–75 to 1975–79. Also the general decrease of subsidence rates after 1979 in the zone of direct contact between the glacier and the rock glacier can be recognized in Figure 9 as vertical acceleration in a mathematical sense. The increasing subsidence rate at lake 5 between 1985–91 and 1991–95 is due to the accelerating growth of this lake (Kääb *et al.*, 1996).

Although changes in elevation did not vary much between 1970 and 1995 with respect to the basic spatial pattern, their variations in time show significant trends. Continuous lowering of the glacier-affected part of Gruben rock glacier as averaged over this entire area indicates, as expected, the existence of dead ice in thermal disequilibrium (Figure 10, bottom). Annual loss in surface elevation (Figure 13, bottom) was decreasing from 1970 to 1979 and increasing again from 1979 to 1991. This development may have been influenced mainly by climatic effects as shown by comparison with variations in surface elevation and net mass balance of the nearby tongue of Gruben glacier (Kääb, 1996), as well as with the variations in net mass balance of Gries glacier (Funk *et al.*, 1997; Figure 14).

In contrast to the continuous lowering of the glacier-affected part of Gruben rock glacier, its periglacial part became thicker from 1975 to 1979 (Figure 10, top). The corresponding annual

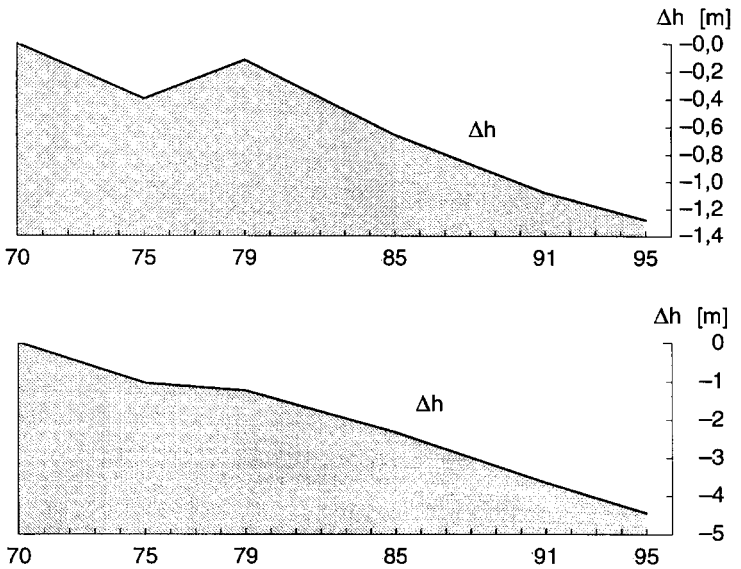

Figure 10 Cumulative change in surface elevation of the periglacial part (top) and the glacier-affected part (bottom). Note the different scales of the two figures.

changes (Figure 13, top) are considerably lower than those of the glacier-affected part, but show some correlation with the above-mentioned glacier mass balance variations as well. This indicates that high-frequency (annual to multi-year) processes of ice loss and ice formation at the permafrost table of the rock-glacier part, and mass balance variations of the nearby glacier, may both be governed by similar climatic parameters.

SURFACE DISPLACEMENTS

The surface displacements of Gruben rock glacier between 1970–75, 1975–79, 1979–85, 1985–91 and 1991–95 were determined using the simultaneous monoplotting technique described above. The raw data were mostly measured at a grid distance of 25 m. Average values of 1970–95 are presented in Figure 11. Accuracy of one single vector is about 0.08 m/a. Again, the velocity field of Gruben rock glacier clearly illustrates differences between the periglacial and the glacier-affected part. From 1970 to 1995, the glacier-affected part with its dead ice at the surface has moved 'back' towards the glacier tongue, with surface velocities reaching up to several metres per year. The highest velocities appear between the thermokarst lake 6 and the glacier-dammed lake 3. The different general direction of surface flow within the glacier-affected part, with respect to the general flow direction within the periglacial part, corresponds to the different directions of maximum surface slope in each of the two areas. Since reliable information on the thickness of the viscously deforming layer is lacking, the exact cause of the velocity maxima observed in Figure 11 remains open. Changes in rheology resulting from differences in ice content and thickness, as well as from slope variations or a combination thereof, are possible explanations. Like the above-mentioned changes in elevation, surface displacements between the thermokarst lake 5 and the glacier tongue also show gradual variations but appear to closely follow gradients in surface slope (Figure 8).

The surface of the periglacial part creeps with velocities of some decimetres per year, but increases sharply to about 1 m/a as the permafrost creeps across and behind the bedrock riegel. This is probably due to combined influences of changes in

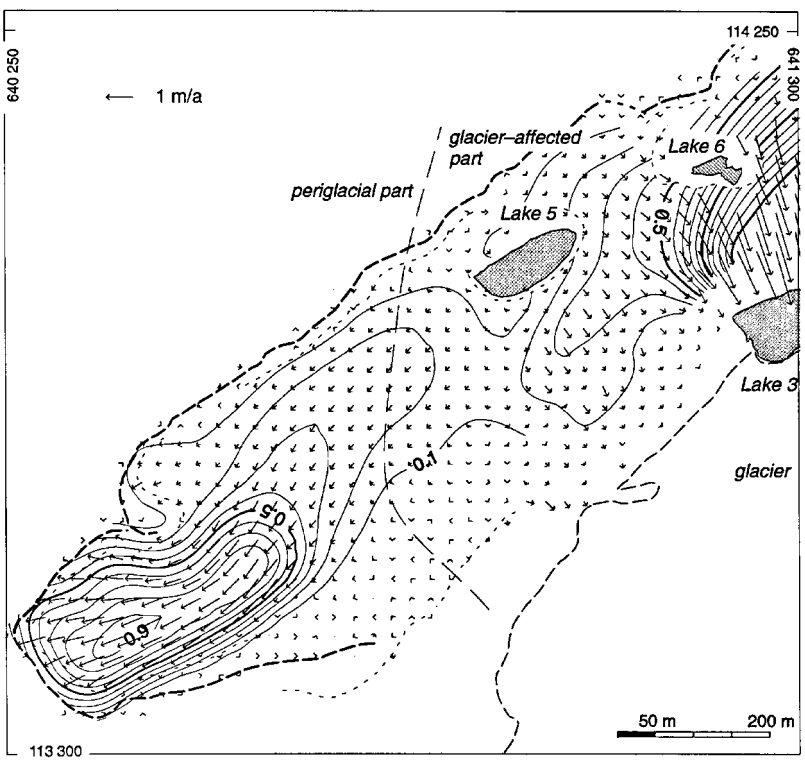

Figure 11 Surface displacements of Gruben rock glacier, 1970–95.

thickness and in surface slope of the frozen material. The lack of deceleration across the little terrace behind the front (at an altitude of about 2820 m; Figure 8) may be the result of stress coupling or thickness variations of the creeping permafrost layer. The area above the bedrock riegel seems to function like a reservoir filled with perennially frozen debris. The debris has mainly accumulated by repeated Holocene glacier advances, but scree from frost weathering in the wall delimiting the rock glacier to the north-west may also be a factor. This mass of ice-rich permafrost is now flowing over its rock dam, forming the main front and a smaller secondary front at the orographic right side.

Figure 13 (bottom) shows the evolution in time of spatially-averaged surface velocities of the whole glacier-affected part of the Gruben rock glacier. The spatial distribution of the temporal changes in horizontal velocity (i.e. the horizontal acceleration or deceleration) is inhomogeneous (Figure 12). Average surface velocities and average elevation changes of the glacier-affected part barely correlate. But in the periglacial part, a clear correlation can be observed (Figure 13, top). Moreover, the spatial distribution of the temporal variations of horizontal and vertical velocities partially correlates (Figures 9 and 12). Although the coupling of changes in elevation and horizontal surface velocities is not surprising, different internal and external causes may be involved.

Assuming constant permafrost creep rates over the last few thousand years, flow lines were calculated for a number of manually selected starting points (Figure 15). The time taken for a particle to travel down the whole length of the rock glacier gives an approximate estimate of the age of the permafrost surface. The central flow lines at the front indicate about 1000–2000 years, but more for the marginal areas. Glacial overriding of the upper rock-glacier parts may have influenced the velocity field and, therefore, the age estimate above. Furthermore, the age of the front surface is not the age of the rock glacier. Comparing the advance

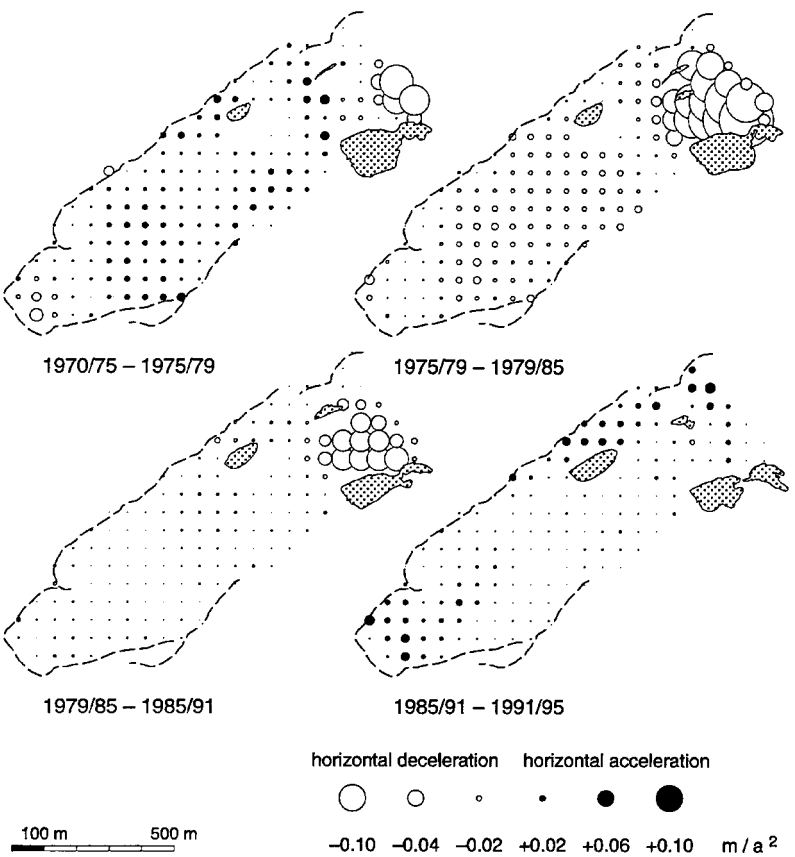

Figure 12 Changes in horizontal surface velocity with time, Gruben rock glacier.

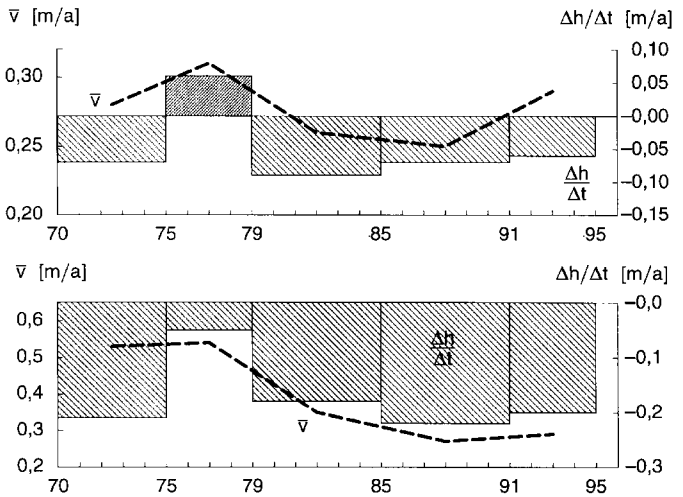

Figure 13 Changes in vertical and horizontal surface velocities of the periglacial part (top) and the glacier-affected part (bottom). Note the different scales of top and bottom figures.

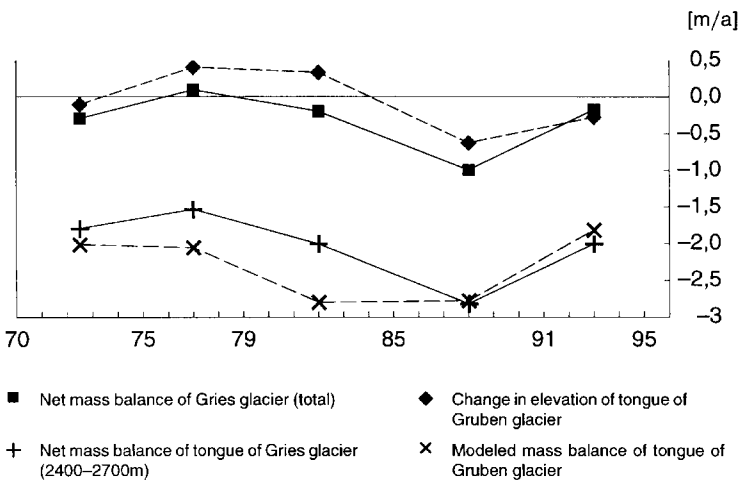

Figure 14 Net mass balance of Gries glacier (Funk *et al.*, 1997) and change in elevation and modelled mass balance of the tongue of Gruben glacier. The changes in surface elevation of the tongue of Gruben glacier are not only caused by the local mass balance, the direct climate signal affecting the rock glacier, but also clearly influenced by changing ice flow. In order to estimate these effects, the local mass balance and the vertical ice flow, both together effecting changes in elevation, have been modelled using the kinematic border condition at the surface (Kääb, 1996).

of the rock-glacier front with the measured surface velocities at selected profiles (Figures 11 and 16) shows that the main front advanced an average distance of 3 m from 1970 to 1995. During the same time interval the surface displacement just above the front totalled 17 m. If the difference is due to (a) the melting of ice within the advancing frozen material and (b) the vertical variation of velocity, rough estimates can be made of average ice contents of the rock-glacier permafrost by assuming characteristic vertical velocity profiles. Talus height at Gruben rock-glacier front is about 30%, indicating some type of internal deformation of the creeping permafrost (Haeberli, 1985; Wahrhaftig and Cox, 1959). With the assumption of 100% basal sliding, the ratio between the mean flow velocity – equalling the surface velocity at the front – and the rate of advance gives a maximum possible average volumetric ice content of up to 85%. On the other hand, assuming a linear velocity profile with depth and a depth-averaged flow velocity equalling half the surface velocity provides a lower estimate of 60–70% by volume. Annual melt rates at the permafrost table within the steep

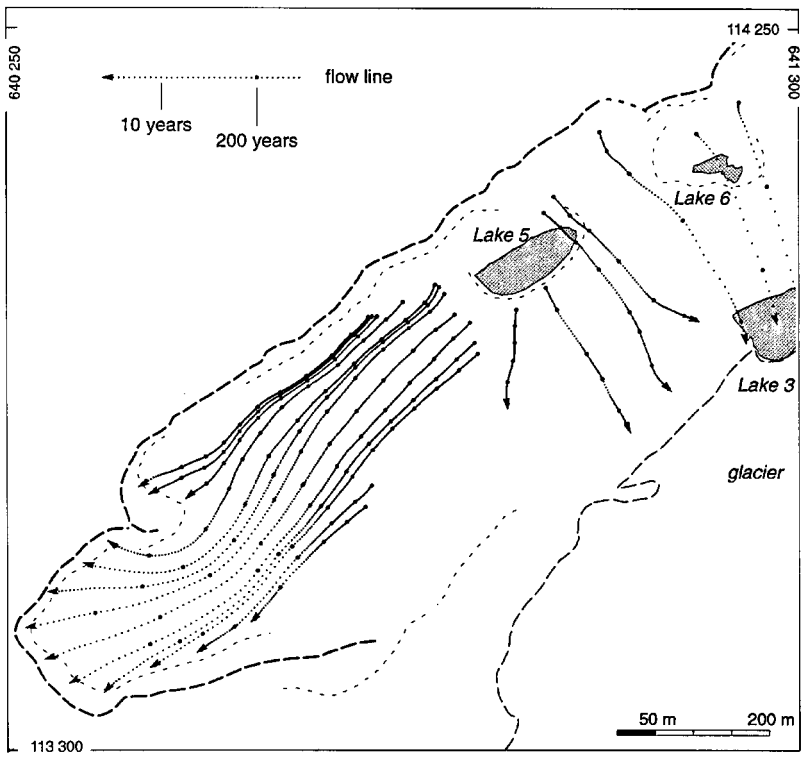

Figure 15 Flowlines interpolated from measured surface displacements assuming a steady state flow field like 1970–95. Small points each represent 10 years, bold points 200 years age difference.

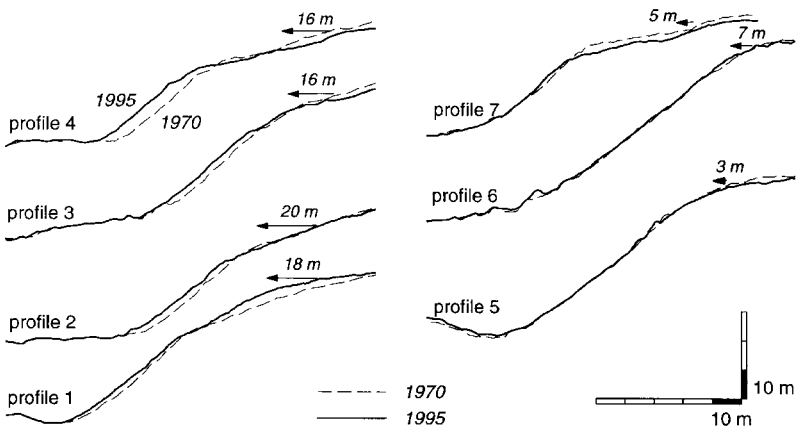

Figure 16 Surface displacement and rock glacier front between 1970 and 1995 at selected profiles (see Figure 3).

front amount to a few decimetres per year. Such values are considerably higher than the measured subsidence rates at the rock-glacier surface but may not be unreasonable for non-permafrost conditions such as they must be expected in the fine-grained rock-glacier front exposed to the sun (south-west). Also, shallow core drillings to a depth of 7 metres and related borehole measurements on the Gruben rock glacier by Barsch *et al.* (1979) gave a volumetric ice content of 90% at the permafrost table, and 50–70% as an average value. Assuming that the ratio of about 15% between the rate of advance and the surface flow velocity has remained constant through time, and integrating this rate over today's flow trajectories, leads to an age estimate for Gruben rock glacier of roughly 10^4 years. The right-lateral front of Gruben rock glacier showed no significant advance between 1970 and

1995 (Figure 16). This points to the complexity of the evolution with locally occurring inactive parts and/or possible intermittent less active stages. In any case, it is reasonable to assume that the rock glacier developed since the end of the last Ice Age through the entire Holocene period.

SURFACE DEFORMATION

Calculation of Surface Strain Rates

The pattern of surface deformation can best be understood by analysing the strain-rate variation at the surface. Strain rates can, in principle, be calculated by applying the expression $\dot{\varepsilon}_{ij} = (v_{i,j} + v_{j,i})/2$ directly to the raw data, but strain rates derived in this way will be sensitive to noise in the data. In fact, the error $\Delta\dot{\varepsilon}_{ij}$ in the strain rates, will, for a given error Δv associated with each velocity determination, increase with the inverse of the spatial distance Δr between data points. For $\Delta r = 25$ m and $\Delta v = 0.035$ m/a, one finds, for example, that $\Delta\dot{\varepsilon}_{ij} = 0.002$ 1/a. This error estimate is larger than most of the expected strain-rate values. Strain-rate variations having longer wavelengths can, however, be determined with a much higher accuracy but they will not be detectable in the noise if the amplitudes of the high-frequency error components are not eliminated or at least reduced significantly. Some kind of error reduction and spatial averaging is imperative if strain rates are to be accurately determined.

The Wiener filter method was used to reduce the velocity errors (Vaseghi, 1996). The velocity distributions $v_x(x, y)$ and $v_y(x, y)$ were transformed into frequency space using the 2D forward Fourier transformation, defined as

$$f(k_x, k_y) = \int_{-\infty}^{+\infty} \int_{-\infty}^{+\infty} f(x, y)\, \mathrm{e}^{i(k_x x + k_y y)}\, \mathrm{d}x\, \mathrm{d}y \quad (1)$$

An optimal Wiener filter

$$W(k) = \frac{|S(k)|^2}{|S(k)|^2 + |N(k)|^2} \quad (2)$$

where $k = \sqrt{(k_x^2 + k_y^2)}$ was determined by constructing a signal model $S(k)$ and a noise model $N(k)$ from the calculated power spectrum of the velocities. The strain rates $\dot{\varepsilon}_{ij}(k_x, k_y)$ were calculated from the noise-reduced velocities by multiplication with wave numbers. As an example, the formula for $\dot{\varepsilon}_{xx}(k_x, k_y)$ was

$$\dot{\varepsilon}_{xx}(k_x, k_y) = -ik_x W(k) v_x(k_x, k_y) \quad (3)$$

The resulting Wiener filter was effectively a low-pass filter with a cutoff at a wavelength of about 100 m. At this wavelength the errors in the strain rates are estimated to be about 0.001 1/a. With increasing wavelengths the errors decrease rapidly.

Surface Strain Rates

Figure 17 shows the pattern of calculated surface strain rates. The arrows represent the horizontal components, and the contour lines the vertical strain rates. Vertical strain rates were calculated from the horizontal ones using the incompressibility condition $\dot{\varepsilon}_{ii} = 0$. There are two regions of high surface strain rates: (1) the front of the periglacial part, in the lower left of Figure 17, and (2) the steep area of the glacier-affected part in the upper right of the figure. The vertical strain rates are generally found to be negative (compression) along the surface, and horizontal strain rates are to a large extent positive (extension). This situation sharply contrasts with the situation on other alpine rock glaciers such as Murtèl and Muragl, where horizontal flow in the lower parts is mostly compressive (e.g. Barsch and Hell, 1976; Vonder Mühll and Schmid, 1993).

Focusing on the front of the periglacial part, it can be seen from Figure 11 that the direction of the flow on the orographic right side changes markedly somewhere close to the point E on Figure 3. The resulting strain-rate pattern can be understood in terms of the general flow characteristics of convergent glacier flow (Gudmundsson, 1994), and can be seen to be the consequence of increasing surface slope towards the front. The flow convergence of the periglacial part at the height of point E shifts the location of the maximum speed towards the left margin and results in a sharp increase in surface flow velocities. This change in the flow regime is the cause of the observed longitudinal extension and the much smaller concomitant transversal compression along the centreline (Figure 17), as well as the transverse extension on the orographic right side. The result is a transverse band of vertical compression with a maximum at the centreline. This flow convergence is followed by a flow divergence as the periglacial part flows past point E, leading to a transverse extension and a

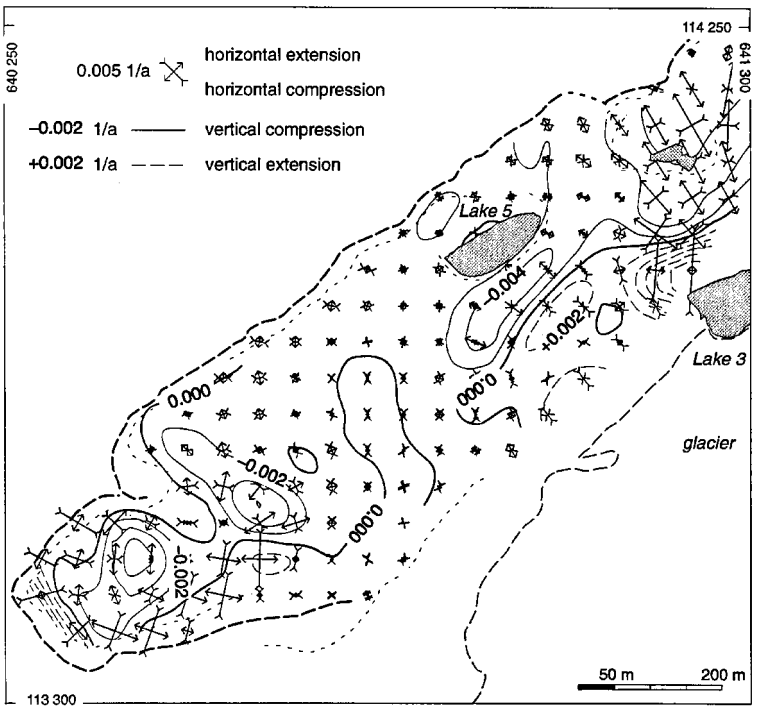

Figure 17 Horizontal principal strain rates 1970–95 at surface, calculated from measured surface displacements. Vertical strain rates 1970–95 at surface, calculated from horizontal strain rates.

corresponding vertical compression. Somewhat surprisingly, the flow velocities increase at the same time, presumably related to an increase in surface slope (see Figure 8).

The increase in surface velocities appears too large to be caused by the horizontal flow convergence alone. The decrease in rock glacier thickness associated with the anticipated bedrock riegel may play some role in shaping the spatial velocity variation. It should also be noted that the surface height variations around the riegel resemble a standing wave of the type predicted from a flow over basal undulations protruding into a deformable medium (Jóhannesson, 1992).

From the north-west margin along the mean flow direction towards the south-east margin of the glacier-affected part, the velocities increase at first as the slope increases, but then in general decrease as the margin is approached. This causes a shift from predominantly extensive to compressive flow. Small deviations from the general pattern (Figure 17) seem to be related to short scale (<100 m) slope variations (see Figure 8).

The gradual spatial variations of strain rates between lake 5 and the glacier margin suggest that the spatial variations in surface elevation are partially affected by ice deformation. The strong vertical extension close to the glacier-dammed lake 3 must be expected to cause vertical thickening of the dead ice over time. In fact, this is the only region (except for the front of the periglacial part, the thickening of which is due to the advance) where a significant increase in height over time can be observed (see Figure 6).

Assuming the average thickness of the creeping permafrost layer to be at least 30 m but not more than 100 m, and the vertical strain rates to decrease linearly with depth, the effective vertical strain at the surface can be estimated. The results show that surface lowering of some cm/a can be the effect of vertical compression. Owing to the predominant vertical compression of the Gruben rock glacier, surface lifting can hardly be explained by vertical strain. On the other hand, the relatively small temporal variations of vertical strain rates between 1970 and 1995 indicate that the changes in elevation observed during the same period may predominantly be affected by climate influences on freezing and thawing processes at the permafrost table rather than by dynamic effects of three-dimensional straining. Freezing and thawing rates at the permafrost base are assumed to have a low frequency and therefore to have little effect on the high-frequency changes in surface elevation.

CONCLUSIONS AND PERSPECTIVES

Techniques of analytical aerophotogrammetry have been applied to monitor the long-term evolution of the Gruben rock glacier, a complex geomorphological feature with both a periglacial and a glacier-affected part. Area-wide velocities and changes in elevation of the rock-glacier surface were determined in order to analyse the creep of mountain permafrost. A 25 year time series at Gruben rock glacier represents the longest of its kind and quality, and provides the following results:

(1) Growth and degradation of permafrost can take place simultaneously at different places within the same rock glacier (see also Haeberli and Schmid, 1988) and can vary at yearly time scales.
(2) Changes in surface elevation within the periglacial part of Gruben rock glacier, during the observation period from 1970 to 1995, reflect overall effects from sediment accumulation/evacuation, three-dimensional deformation, and freezing and thawing processes. Measured values lie in the range ± 10 cm/a. Surface lowering prevails with an average value of -5 cm/a. In the glacier-affected part, which still has some buried ice, surface lowering is considerably higher and averages -0.2 m/a.
(3) Surface velocities reach values of 1 m/a and show changes of up to 20% within a few years.
(4) For the investigated period, temporal changes in surface elevation do not correlate with temporal changes in surface strain regime. The latter shows no significant variations in time. Long-term surface lowering can be related, however, to the observed overall vertical compression at the surface of about -0.002 1/a (maxima of up to -0.006 1/a). Thus, only part of the measured surface subsidence is assumed to be due to thawing.
(5) Short-term variations of vertical surface changes appear to be coupled with synchronous variations in horizontal flow velocities. This photogrammetrically documented time series shows some similarity with mass balance variations of the nearby Gruben and Gries glaciers. Possibly, this is a consequence of common climatic forcing (summer temperature?).
(6) Between 1970 and 1995, the front of Gruben rock glacier advanced about 10 cm per year, about 0.15 times the surface velocity. Assuming a steady state flow field, the surface of the rock glacier can be estimated to be 1000–2000 years old. Assuming a constant advance rate of 0.15 times the surface velocity, the Gruben rock glacier as a whole can be estimated to have developed and advanced during the Holocene.

The correlation between the three-dimensional geometrical behaviour of Gruben rock glacier and different glacier mass balance variations shows that the long-term observation of rock-glacier kinematics could provide interesting signals of climate effects on mountain permafrost. In order to understand these signals, as reflected by rock-glacier behaviour, it is necessary to monitor and model the energy balance of mountain permafrost.

In view of the inhomogeneous internal structure of the permafrost body and the complex processes taking place at the permafrost base and the permafrost table, improved physical modelling is required to understand the dynamic behaviour of creeping mountain permafrost. Combining high-precision and area-wide surface information from photogrammetry with depth information from drillings and geophysical soundings seems to be most promising for collecting an adequate data base for this purpose.

ACKNOWLEDGEMENTS

The present study was carried out as part of the Swiss National Research Programme 31 on Climate Change and Natural Disasters through project 4031-34232 with funds of the Swiss National Science Foundation. The photogrammetric investigations are based on the aerial photographs taken by the Federal Office of Cadastral Surveys (Eidgenössische Vermessungsdirektion). Special thanks are due to M. Hoelzle and D. Vonder Mühll for critically reading the manuscript.

REFERENCES

Armenakis, C. (1984). Deformation measurements from aerial photographs. *Int. Archives of Photogrammetry and Remote Sensing*, **XXV**(A5), 39–48.

Barsch, D. and Hell, G. (1976). Photogrammetrische Bewegungsmessung am Blockgletscher Murtèl I, Oberengadin, Schweizer Alpen. *Zeitschrift für Gletscherkunde und Glazialgeologie*, **11**(2), 111–142.

Barsch, D., Fierz, H. and Haeberli, W. (1979). Shallow core drilling and borehole measurements in permafrost of an active rock glacier near the Grubengletscher,

Wallis, Swiss Alps. *Arctic and Alpine Research*, **11**(2), 215–228.

Evin, M. and Assier, A. (1982). Mise en évidence du mouvement sur le glacier rocheux du Pic d'Asti (Queyras, Alpes du Sud, France). *Revue de Géomorphologie Dynamique*, **31**(4), 127–136.

Finsterwalder, R. (1931). Geschwindigkeitsmessungen an Gletschern mittels Photogrammetrie. *Zeitschrift für Gletscherkunde und Glazialgeologie*, **19**, 251–262.

Funk, M., Morelli, R. and Stahel, W. (1997). Mass balance of Griesgletscher 1961–1994: different methods of determination. *Zeitschrift für Gletscherkunde und Glazialgeologie*, **33**(1), 41–56.

Grün, A. and Sauermann, H. (1977). Photogrammetric determination of time-dependent variations of details of a glacier surface using a non-metric camera. In *Symposium on Dynamics of Temperated Glaciers and Related Problems, München*.

Gudmundsson, G. H. (1994). Converging glacial flow – a case study: the Unteraarglacier. *Mitteilungen der Versuchsanstalt für Wasserbau, Hydrologie und Glaziologie der ETH Zürich*, **131**.

Flotron, A. (1979). Verschiebungsmessungen aus Luftbildern. *Mitteilungen der Versuchsanstalt für Wasserbau, Hydrologie und Glaziologie der ETH Zürich*, **41**, 39–44.

Haeberli, W. (1980). Morphodynamische Aspekte aktueller Gletscherhochwasser in den Schweizer Alpen. *Regio Basiliensis*, **21**(3), 58–78.

Haeberli, W. (1985). Creep of mountain permafrost. *Mitteilungen der Versuchsanstalt für Wasserbau, Hydrologie und Glaziologie der ETH Zürich*, **77**.

Haeberli, W. and Schmid, W. (1988). Aerophotogrammetrical monitoring of rock glaciers. In: *Proceedings, Fifth International Conference on Permafrost*, Trondheim, Norway. Vol. 1, pp. 764–769.

Haeberli, W. and Vonder Mühll, D. (1996). On the characteristics and possible origins of ice in rock glacier permafrost. *Zeitschrift für Geomorphologie N.F., Suppl.-Bd.*, **104**, 43–57.

Haeberli, W., King, L. and Flotron, A. (1979). Surface movement and lichen-cover studies at the active rock glacier near the Grubengletscher, Wallis, Swiss Alps. *Arctic and Alpine Research*, **11**(4), 421–441.

Haeberli, W., Hoelzle, M., Keller, F., Schmid, W., Vonder Mühll, D. S. and Wagner, S. (1993). Monitoring the long-term evolution of mountain permafrost in the Swiss Alps. In: *Proceedings, Sixth International Conference on Permafrost*, Beijing, China. Vol. 1, pp. 214–219.

Hofmann, W. (1958). Bestimmung von Gletschergeschwindigkeiten aus Luftbildern. *Bildmessung und Luftbildwesen*, **3**, 71–88.

Jóhannesson, T. (1992). *Landscape of Temperate Ice Caps*. PhD thesis, University of Washington.

Kääb, A. (1996). Photogrammetrische Analyse zur Früherkennung gletscher- und permafrostbedingter Naturgefahren im Hochgebirge. *Mitteilungen der Versuchsanstalt für Wasserbau, Hydrologie und Glaziologie der ETH Zürich*, **145**.

Kääb, A. and Haeberli, W. (1996). Früherkennung und Analyse glazialer Naturgefahren im Gebiet Gruben, Wallis, Schweizer Alpen. *Tagungspublikation Interpraevent 1996*, **4**, 113–122.

Kääb, A., Haeberli, W. and Teysseire, P. (1996). Entwicklung und Sanierung eines Thermokarstsees am Gruben-Blockgletscher (Wallis). *Berichte und Forschungen. Geographisches Institut. Universität Freiburg/CH*, **8**, 145–153.

Kaufmann, V. (1996). Der Dösener Blockgletscher – Studienkarten und Bewegungsmessungen. *Arbeiten aus dem Institut für Geographie der Karl-Franzenz-Universität Graz, Beiträge zur Permafrostforschung in Österreich*, **33**, 141–162.

King, L., Fisch, W., Haeberli, W. and Waechter, H. P. (1987). Comparison of resistivity and radio-echo soundings on rock-glacier permafrost. *Zeitschrift für Gletscherkunde und Glazialgeologie*, **23**(1), 77–97.

Messerli, B. and Zurbuchen, M. (1968). Blockgletscher im Weissmies und Aletsch und ihre photogrammetrische Kartierung. *Die Alpen, SAC*, **3**, 139–152.

Röthlisberger, H. (1979). Glaziologische Arbeiten im Zusammenhang mit den Seeausbrüchen am Grubengletscher, Gemeinde Saas Balen (Wallis). *Mitteilungen der Versuchsanstalt für Wasserbau, Hydrologie und Glaziologie der ETH Zürich*, **41**, 233–256.

Saksono, T. (1984). *Combination of Single Photographs and Digital Height Models for Planimetric and Height Data Extraction*. Ohio State University.

Vaseghi, S. V. (1996). *Advanced Signal Processing and Digital Noise Reduction*. Wiley, Chichester.

Vonder Mühll, D. S. and Schmid, W. (1993). Geophysical and photogrammetrical investigation of rock glacier Muragl I, Upper Engadin, Swiss Alps. In: *Proceedings, Sixth International Conference on Permafrost*, Beijing, China. Vol. 1, pp. 214–219.

Vonder Mühll, D. S., Haeberli, W. and Klingelé, E. (1996). Geophysikalische Untersuchungen zur Struktur und Stabilität eines Moränendammes am Grubengletscher (Wallis). *Tagungspublikation Interpraevent 1996*, **4**, 123–132.

Wagner, S. (1992). Creep of alpine permafrost, investigated on the Murtèl rock glacier. *Permafrost and Periglacial Processes*, **3**(2), 157–162.

Wagner, S. (1996). Dreidimensionale Modellierung zweier Gletscher und Deformationsanalyse von eisreichem Permafrost. *Mitteilungen der Versuchsanstalt für Wasserbau, Hydrologie und Glaziologie der ETH Zürich*, **146**.

Wahrhaftig, C. and Cox, A. (1959). Rock glaciers in the Alaska Range. *Geological Society of America Bulletin*, **70**, 383–436.

